Progress In Electromagnetics Research C, Vol. 81, 63–75, 2018

A High Return Loss of Microwave Bandpass Filter Using Superconducting Electrospun YBCO Nanostructures

Saleh E. Jasim[1, 2], Mohamad A. Jusoh[1, *], You Kok Yeow[3], and Jose Rajan[1]

Abstract—A high return loss (−30 dB), small size (100 mm^2) and broad bandwidth (1.5 GHz) microwave bandpass filter has been designed using finite element modelling and practically realized using superconducting $YBa_2Cu_3O_{7-\delta}$ (YBCO) thin films deposited on a (10×10 mm^2) $LaAlO_3$ substrate by spin coating. Superconducting YBCO material was prepared by electrospinning technique and solid-state reaction. The microwave properties of filter circuits were experimentally determined using the vector network analyser (VNA) at room temperature (300 K) and in the presence of liquid nitrogen (77 K). The solid-state filter showed high return loss (i.e., −22 dB) at operating frequency of 9.7 GHz and broad bandwidth of 1.5 GHz, which is consistent with the simulation results. The insertion losses for YBCO filters are ~ -2, ~ -1.5 and ~ -3 dB for the normal, nanoparticle and nanorod respectively. However, the electrospun filters exhibited lower performance due to the nano-structural properties of YBCO samples at nanoscale which make these samples have a large band gap compared to solid-state sample. The results indicate that the filter design and simulation result are reliable. Hence, HTS YBCO could be a potential microwave bandpass filter in industry.

1. INTRODUCTION

Development of superconducting microwave passive circuit components, such as low loss and broad bandwidth bandpass filters, is an active area of research for the selection of the high-fidelity signal within the broadcast radio in radio frequency (RF) and microwave communication systems [1–3]. Generally, the electrical performances of the filters are described in terms of insertion loss, return loss, and frequency-selectivity (i.e., attenuation at rejection band) [4]. Filters should have small insertion loss, large return loss for good impedance matching with interconnecting components, and high frequency-selectivity to prevent the interference and high performance. A number of reports have been published on the superconducting microwave circuits such as antenna, filter, phase shifter, multiplexer, coupler and delay lines with high performance and low cost [5, 6].

High-temperature superconductor HTS $YBa_2Cu_3O_{7-\delta}$ (YBCO) is characterized by several unique properties to be used as a microwave filter material, such as lower RF losses than conventional conductors [5–7]; many bandpass filters are designed using HTS YBCO thin films with several types of lumped elements, such as four-pole cross-coupled [8], compact eight-pole [9] and parallel-connected network [10]. However, most of the reported bandpass filters employed large area ($\sim$ 225–5900 mm^2). Recently, nanoscale superconductivity is gaining popularity because of many fundamental and technological advantages at such length scales such as high surface to volume ratio, size induced modification in optical and electronic properties, high mechanical strength, and lightweight. Usually wet-chemical methods, such as template method, sol-gel, and anodization, are used for preparing

Received 26 October 2017, Accepted 28 November 2017, Scheduled 4 February 2018

* Corresponding author: Mohamad Ashry Jusoh (ashry@ump.edu.my).

[1] Faculty of Industrial Sciences & Technology, Universiti Malaysia Pahang, Gambang Kuantan, Pahang 26300, Malaysia. [2] Technical Institute, Hawija, Northern Technical University, Hawija, Kirkuk 36007, Republic of Iraq. [3] Faculty of Electrical Engineering, Universiti Teknologi Malaysia, Skudai, Johor 81310, Malaysia.

nanoscale superconducting YBCO but with poor scalability. In this context, nanomaterial fabrication using a polymeric solution and electric fields based continuous nanofiber production method, called electrospinning, offers scalable production [11–15]. We have now developed broadband bandpass filters with a small size (100 mm^2) and high return losses using HTS YBCO nanostructure thin films prepared by electrospinning process. The filter was designed and modelled under finite element modelling using HFSS software [16].

2. EXPERIMENTAL PROCEDURE

2.1. Filter Design

In this work, a microwave filter is designed to allow the central frequency 10.0 GHz to pass through and attenuate other frequencies outside. The microwave filter is designed with a parallel coupling line model. There are several ways to create a coupling resonator between the microstrip lines. The basic principle to design the coupled lines is that the two microstrip lines must be parallel at least at sub-sections of the length of two microstrip lines. The coupled lines of the microwave filter were designed with four parallel tapes which were assigned as a perfect conductor (see Figure 1). The microwave filter is designed using a ($10 \times 10\,mm^2$) $LaAlO_3$ substrate, which is assigned as a dielectric material with dielectric constant 23.5, and further information for filter design can found in last work [16].

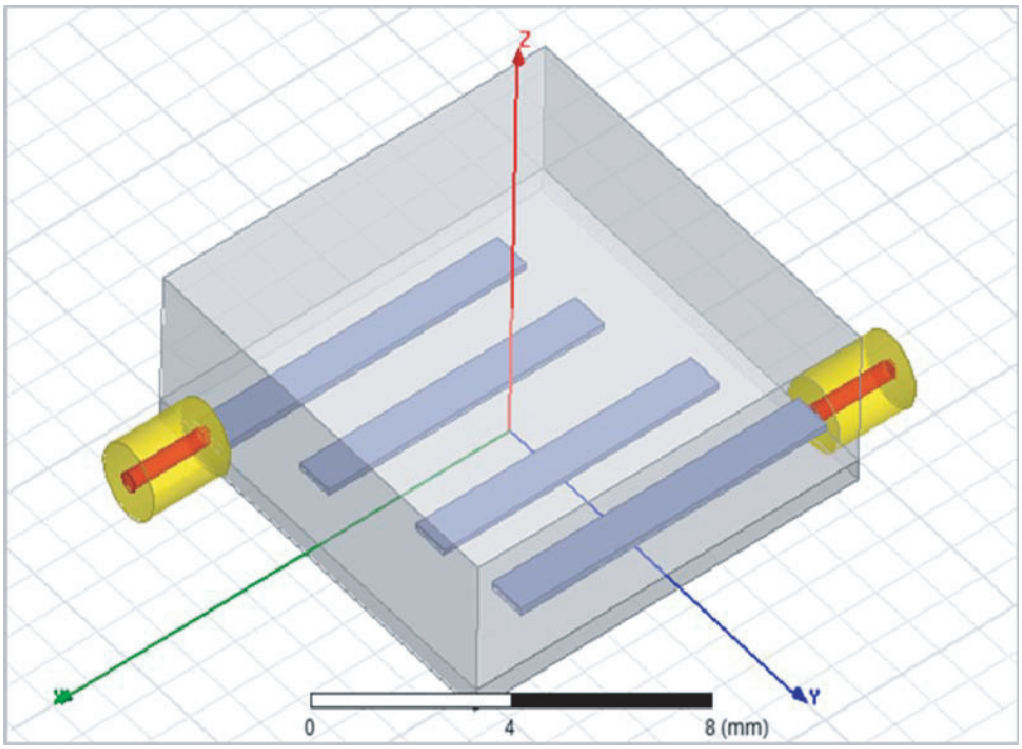

Figure 1. The image of the designed microwave bandpass filter circuit from the HFSS software.

The HTS YBCO nanostructure was prepared by an electrospinning process, the details of which are reported elsewhere [17]. The morphology of the samples was observed using Field Emission Scanning Electron Microscope (FESEM, JEOL, model: JSM-7600) operating at 5.0 kV. The crystal structure of the annealed samples was analyzed by X-ray diffractometer (Rigaku, model: Miniflex II, CuKα, 30 kV, 15 mA). The transition temperatures (T_c) of the samples were determined using an AC Susceptometer of a closed cycle liquid helium refrigeration system (Cryo Industry model REF-1808-ACS). The surface area of the samples was measured using BET Surface Area and Porosity Analyzer (Micrometrics, model: ASAP 2020). The samples were degassed at $\sim 400°C$ for 7 h before the adsorption measurements.

2.2. Filter Fabrication

In this section, the YBCO thin films were deposited properly employing the spin coating technique using the nanostructure powder prepared by the electrospinning process as well as using the powder of YBCO prepared by the solid-state reaction method. The designed circuit of microwave filters was transferred from the HFSS software to the AutoCAD software. The circuit was then printed on a heat-transfer paper (photo laser paper) by the laser printer. The etching process was applied to remove the unwanted parts of the thin film (leaving only the required designed circuit). The heat treatment process was conducted to increase the stability of the printed circuit, increase the oxygen content and remove the solvent and other impurities that might adhere to the sample during the etching process. The second deposition was then made to produce the thin film of the ground plane for the microwave filter samples. Finally, heat treatment was performed on the samples (in oxygen atmosphere) to increase the oxygen content. High oxygen content would increase the performance of YBCO. The device fabrication process is schematically shown in Figure 2, which describes the representation of the heat-transfer paper of the printed circuit on the thin film step by step.

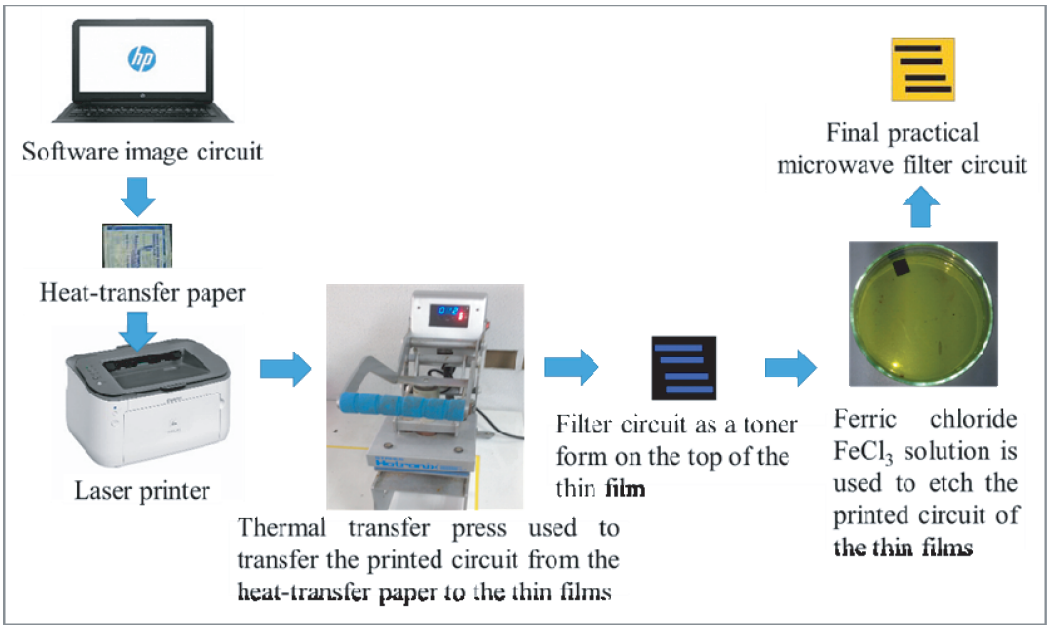

Figure 2. The graphic flow chart displays the three steps followed to transfer the filter circuit from the software to the thin film of the sample using the heated transfer paper and the toner.

3. RESULTS AND DISCUSSION

3.1. Simulation Results

The performance of a designed filter can be summarized in terms of the return and insertion losses for the selected frequency — an ideal filter should have high return loss, low insertion loss, broad bandwidth, good impedance matching and high frequency selection. Figure 3 presents the simulated results of the designed device using HFSS software. The simulation results display the response between the scattered S-parameters (S_{11} reflection coefficients and S_{12} transmission coefficient in dB) and the frequency in GHz.

In general, the results of simulation of a filter depend on line width, line height, line coupling length, and the distance between the lines [18, 19]. As can be seen from Figure 1, the optimized filter has an operation frequency of $\sim$ 10 GHz with a bandwidth of $\sim$ 1.5 GHz, transmission frequencies in the 9.5–10.9 GHz range, a return loss more than -20 dB, and approximately no insertion losses. On

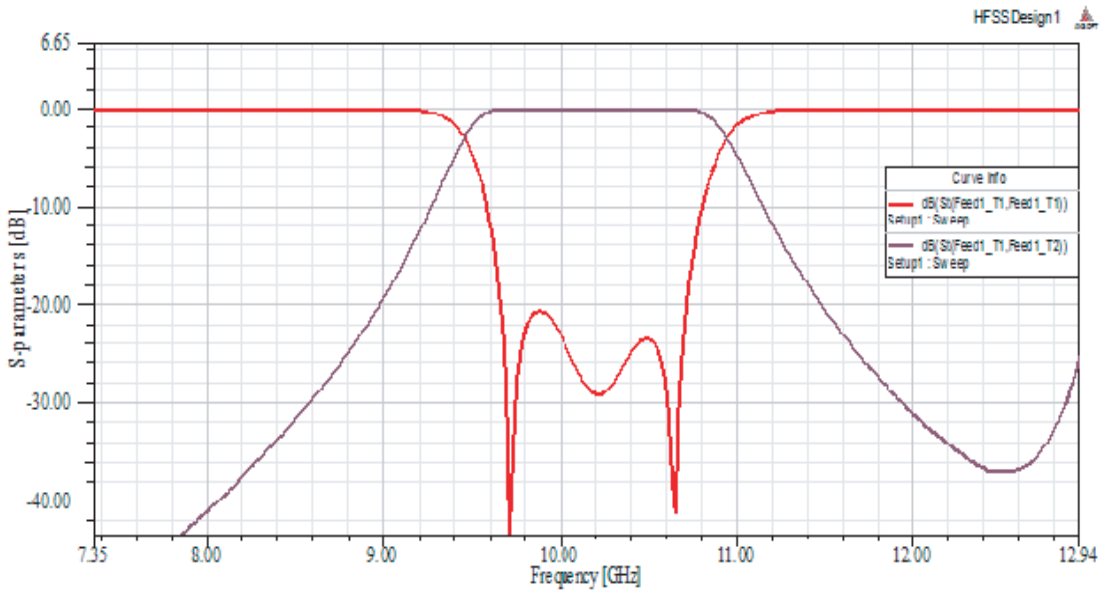

Figure 3. HFSS plot of the S-parameters versus frequency with frequency center 10.2 GHz.

the other hand, Kumar et al. [20] recently designed microwave filter using finite modelling with 4-parallel coupled line pairs with a spacing < 1 mm apart using the HFSS software. These filters, on the FR4 substrate (which is a composite material composed of flame-resistant woven fiberglass cloth with an epoxy resin binder) of dielectric constant ~ 4.2 and thickness ~ 1.58 mm, gave much inferior performance (operating frequency ~ 2.48 GHz, bandwidth ~ 0.6 GHz, high insertion loss ~ 2.2 dB, and low return loss ~ -12 dB). On the other hand, we have undertaken an extensive optimization procedure in the present work that yielded high performance with wide bandwidth and high return loss for couple line distance > 1 mm. In the following, we describe the experimental results on the morphology, structure and superconducting of the electrospun YBCO nanoparticles, and the characteristics of the microwave filter employing the above design. The properties of the electrospun YBCO particles have been benchmarked with the filter fabricated using materials obtained by conventional solid-state reaction process.

3.2. Characterization Results

Figure 4 summarizes the morphology of the samples used for fabrication of the microwave filters. The SEM images (top panel) showed agglomerated nanoparticles of size in the 200–400 nm range, and the agglomeration most likely results from the high-temperature heat treatment involved. A closer examination revealed that agglomerates contain finer particles of size ~ 50 nm. The SEM images in the bottom panel show the morphology of the nanorods (NRs) electrospun sample having average diameter ~ 75 nm and length ~ 900 nm.

Figure 5 shows the crystal structure of the fabricated YBCO samples using the solid-state and electrospinning routes; the XRD pattern shows that the peaks can be indexed to the orthorhombic structure with lattice constants $a = 3.897$ Å, $b = 3.8889$ Å, $c = 11.707$ Å, $V = 177.4064$ Å^3 and corresponds to the superconducting phase [12, 13]. The Tc measurements of YBCO samples were conducted using AC susceptibility techniques of a closed cycle liquid helium refrigeration; the result of AC susceptibility measurements is consistent with the conventional four-probe technique [21, 22].

Figure 6 shows the AC susceptibility as a function of the temperature of the samples; the T_c of the YBCO samples was estimated from these curves were in the 82–92 K range. The complex susceptibility (χ) consists of the real and imaginary parts ($\chi = \chi + i\chi$). The real part (χ) of susceptibility shows a sudden decrease as the temperature decreased after the TC, whereas the imaginary part (χ) increases gradually with temperature after T_c. The decrease in the real part is attributed to the diamagnetic properties of the samples, whereas the increase in the imaginary part represents the AC losses for samples prepared by solid-state and electrospinning process, respectively [22].

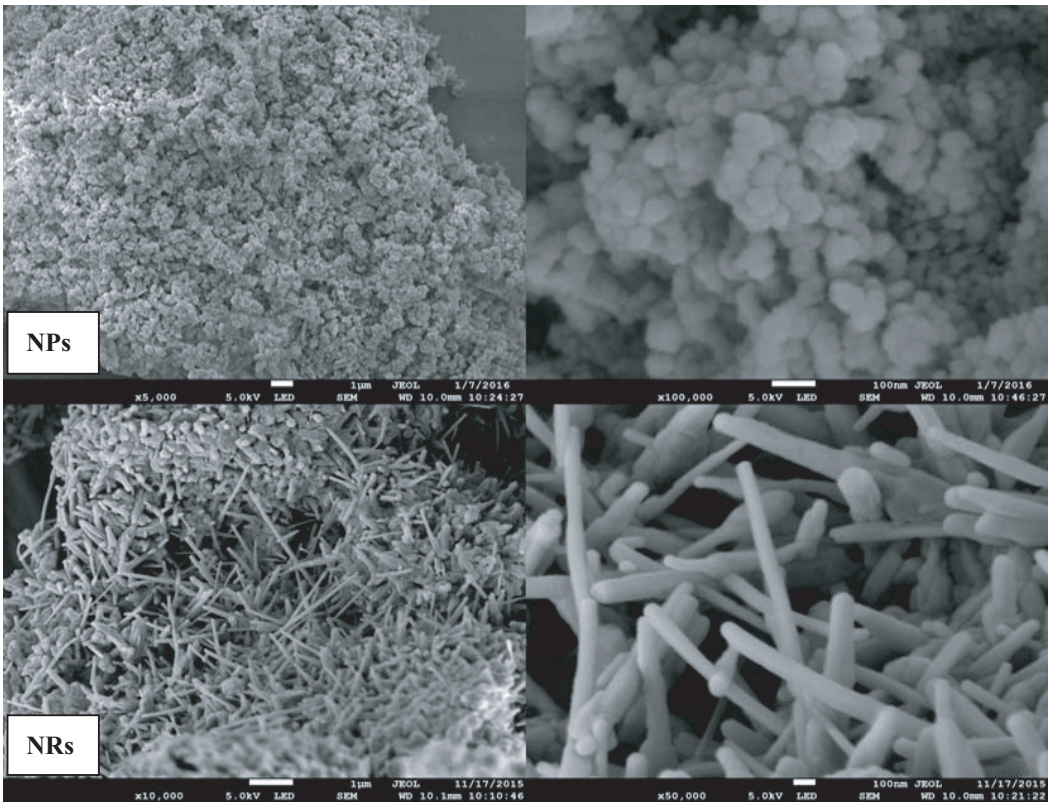

Figure 4. FESEM images of HTS YBCO nanostructures synthesized using electrospinning method.

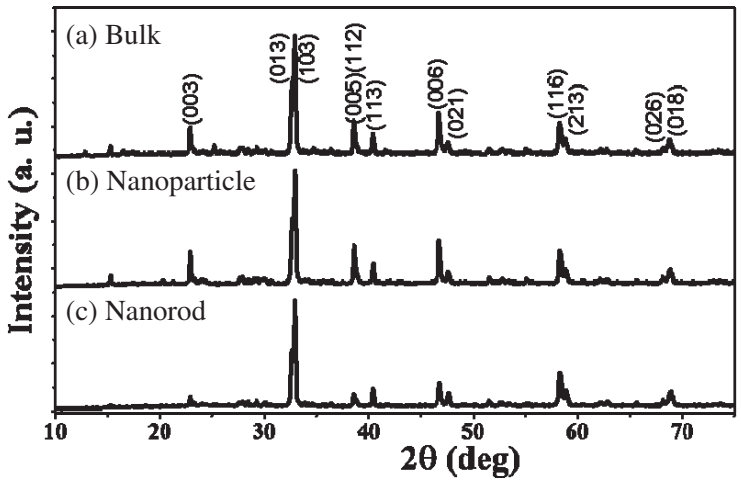

Figure 5. X-ray diffraction pattern of the HTS YBCO synthesized using electrospinning process and solid-state reaction method. (a) Bulk. (b) Nanoparticle (NPs). (c) Nanorod (NRs).

3.3. Filter Measurement

The Vector Network Analyzer (VNA, Model E5071C, 300 kHz–20 GHz, Agilent Technology) was used to test the performance of the devices. The experimental setup used to test the performance of the filters consisted of VNA, coolant box, sample holder and fabricated bandpass filter. The sample was connected to SMA connectors using the sample holder. This holder was designed to connect the ground plane of the filter with the aluminum plate in order to produce a perfect electric/thermal conductor. The

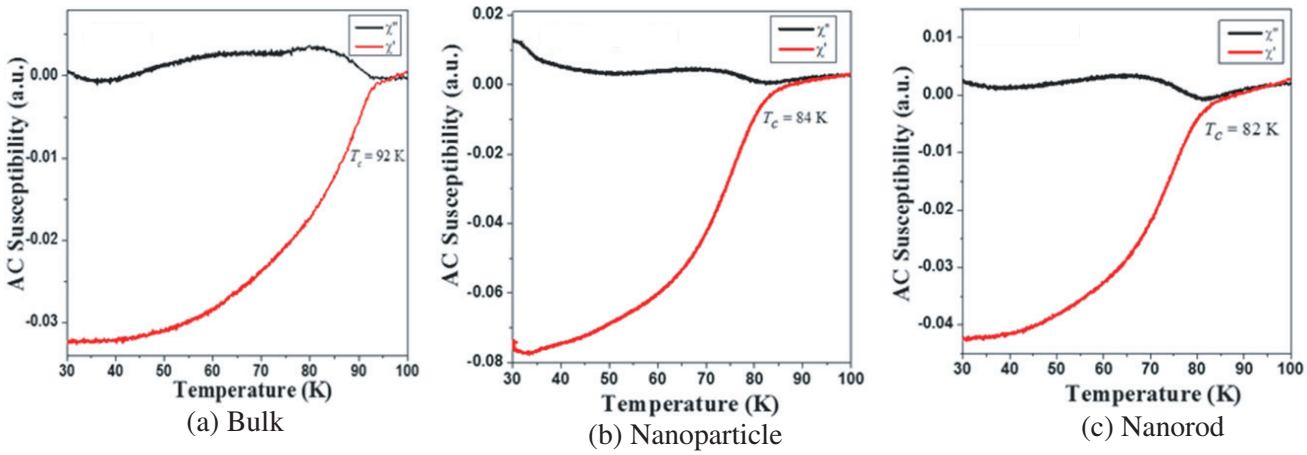

Figure 6. AC Susceptibility ($\chi = \chi + i\chi$) measurements versus temperature of YBCO samples. (a) Bulk. (b) Nanoparticle (NPs). (c) Nanorod (NRs).

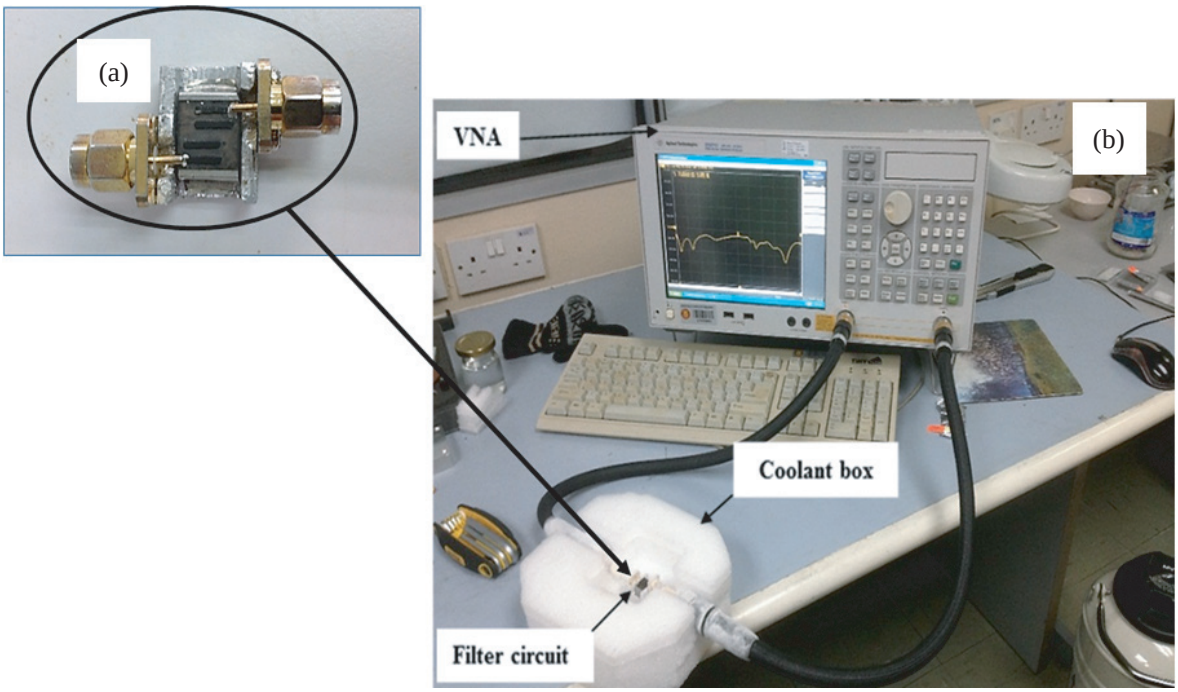

Figure 7. (a) The layout of the bandpass filter with four couple parallel line. (b) Experimental setups for transmission and reflection coefficients measurements of HTS YBCO bandpass filter.

two conductive terminals of VNA were calibrated using the full two-port SOLT method to eliminate all instrumentation errors. The measurements were carried out at frequency ranging from 8 GHz to 12 GHz for both temperatures, i.e., 300 K (room temperature) and 77 K. Figure 7 shows the experimental setup for transmission and reflection coefficients measurements of HTS YBCO filter, VNA, and liquid nitrogen mini Coolant system.

Here, the variations of S-parameter at different frequencies are presented. For each sample, both reflection coefficient (S_{11}) and transmission coefficient (S_{12}) are discussed. For clarity purpose, a framework explaining the presence of filter results is illustrated in Figure 8.

The bandpass filter was fabricated from two types of YBCO thin films prepared by electrospinning and solid-state processes. Via electrospinning, two kinds of morphologies (i.e., nanorod and

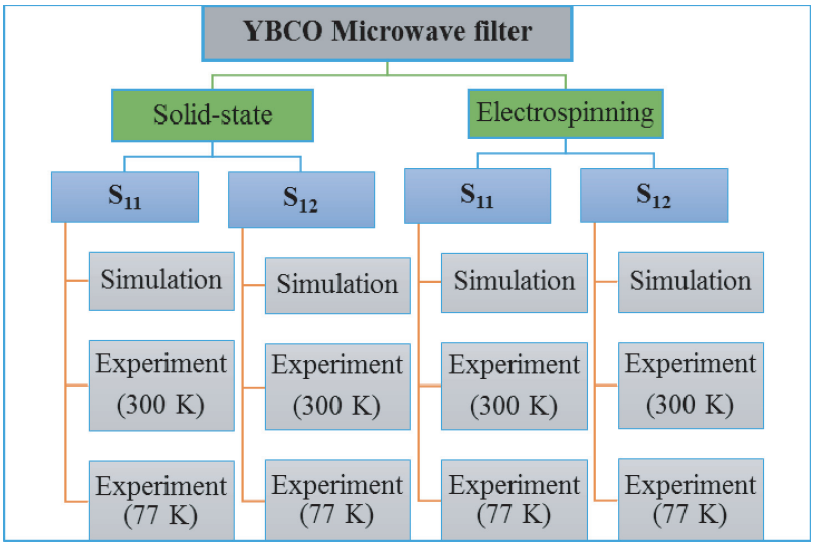

Figure 8. Framework to display the simulation and experiment results of the designed and fabricated filters.

Table 1. The samples morphology and synthesis process of the designed filters.

Filter Name	Morphology	Synthesis process
A	Normal structure	Solid state
B	Nanoparticle	Electrospinning
C	Nanorod	Electrospinning

nanoparticle) were formed. The details of the designed filters such as morphology and synthesis process are listed in Table 1.

3.4. Filter Response

Figure 9 summarizes the simulated and experimental results of the frequency response characteristics of the microwave filter using YBCO thin film prepared from solid-state reaction. The reflection coefficient (S_{11}) differs from the transmission coefficient (S_{12}) considerably at 300 K and 77 K as illustrated in panel (a) by the left (S_{11}) and right (S_{12}) panel (b) of Figure 6, thus, revealing the role of superconductivity in the microwave characteristics. The return loss was calculated from S_{11} (left panels), and insertion loss was calculated from S_{12} (right panels). The filter made from the solid-state reaction (77 K) showed return losses of -22 dB and -15 dB at frequencies $\sim$ 9.7 GHz and 10.8 GHz, respectively. Therefore, the return loss is lower than the simulated response of S_{11}. No response was observed at 300 K. It is interesting to note that the experimental response is very similar to the simulated one. Filter (A) showed lower return loss than the simulated one, mainly due to the mismatches and resistance between the contact pads and the electrical contact, which were probably affected by dipping the filter into the liquid nitrogen).

On the other hand, the S_{11} responses in the spectrums of microwave Filters B and C made from the thin film of the electrospun YBCO nanostructures are shown in the left panels. The average return losses are -15 dB at $\sim$ 10.2 GHz and -12 dB at 10.3 GHz, which showed lower return loss than the simulated responses of S_{11} shown in Figure 10 and Figure 11 (left panel (a) and right panel (b)). This result is consistent with that work reported by Zhang et al. [23], who have synthesized the filter using YBCO thin film, where an Au thin film was deposited on top of the YBCO thin film. Their measured return loss results of the S_{11} response were also less than the simulation ones.

However, this could be attributed to the sample structure, for YBCO at the nanoscale (high

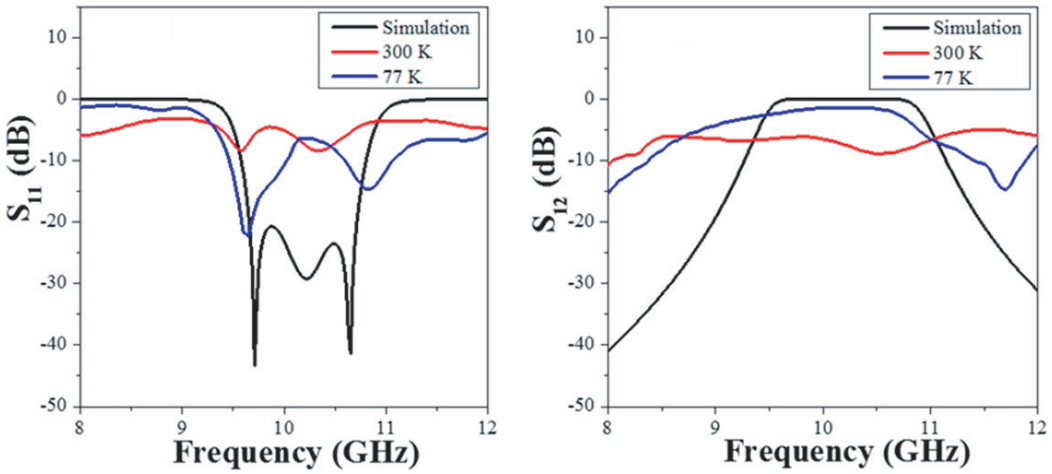

Figure 9. Simulation and experiment results of (Sample A) YBCO microwave bandpass filter prepared by solid-state reaction method, measured using VNA at temperature 300 and 77 K. (a) S_{11} response. (b) S_{12} response.

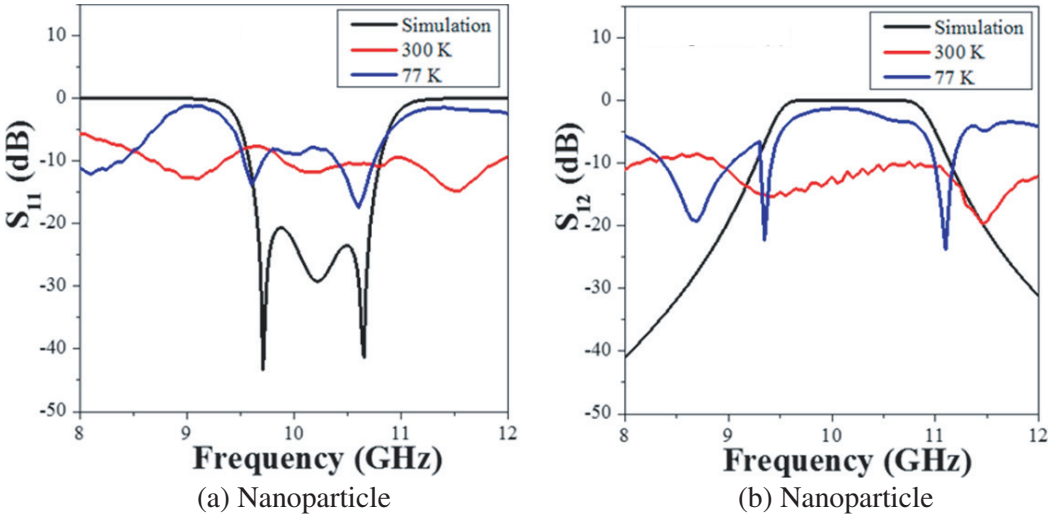

Figure 10. Simulation and experiment results of (Sample B) YBCO microwave bandpass filter prepared by electrospinning process, measured using VNA at temperature 300 and 77 K. (a) S_{11} response. (b) S_{12} response.

surface area, increased the band gap), which was lastly improved by [24], which investigated the effect of doping nanomaterial in pure YBCO as well. Besides, in the study of [25], the authors investigated the superconducting properties at the nanoscale. These properties were dependent on confining geometry and shapes. The oscillatory behavior of the superconducting property is consistent with the current finding. The current results are consistent with those reported in [24, 25]. It is important to mention here that perfect insulator (with homogeneous property) was adopted in the simulation. Moreover, different properties of the material were used in simulation, and it is a quite perfect conductor compared to measured results. It is also because the simulation process did not consider the structure of the material and only considered the perfect conductor and homogeneous material.

The insertion losses for YBCO filters calculated from S_{12} (in right panels) are ~ -2, ~ -1.5 and ~ -3 dB for the normal, nanoparticle and nanorod, respectively. The electrospun YBCO nanoparticles show much lower insertion loss than that of Lu et al.'s work [26]. The resulting bandwidth of the bulk

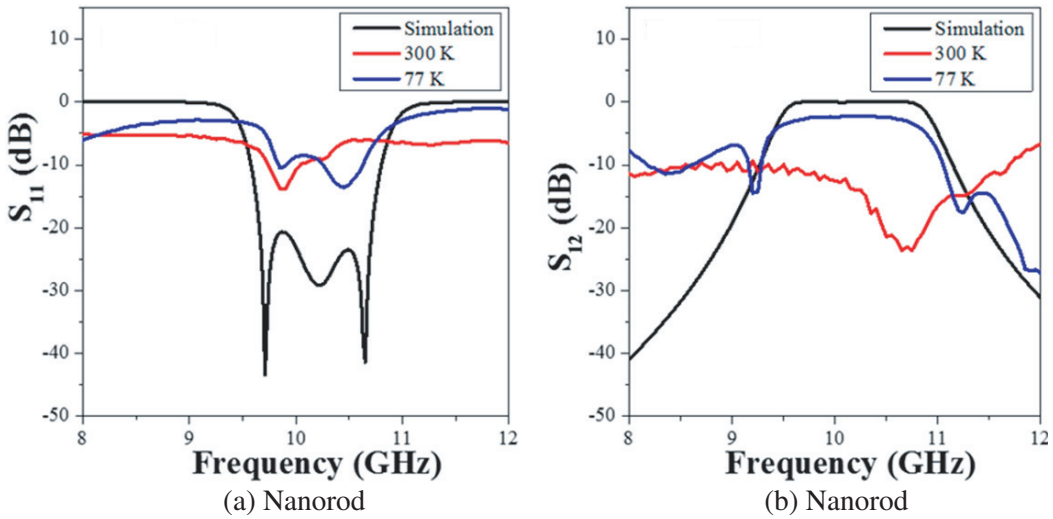

Figure 11. Simulation and experiment results of (Sample C) YBCO microwave bandpass filter prepared by electrospinning process, measured using VNA at temperature 300 and 77 K. (a) S_{11} response. (b) S_{12} response.

Table 2. Response of the YBCO microwave bandpass filter samples.

NO.	Filter Sample	Bandwidth (GHz)	Return loss (dB)	Insertion loss (dB)
1	A	2.0	−22	−2.0
2	B	1.5	−15	−1.5
3	C	1.5	−12	−3.0

filter is more than 1.5 GHz, while the nanostructured YBCO filters bandwidths are similar at 1.5 GHz, which is consistent with the simulated result. The agreement is due to the low losses of YBCO sample at high frequency. Hence, the broad bandwidth of YBCO filters can be produced. Table 2 summarizes the characteristic results of each filter made from the three kinds of YBCO thin films prepared by solid-state reaction and electrospinning process.

4. RESULT ANALYSIS OF THE DESIGNED FILTERS

The response of the electrospun YBCO filters is consistent with the simulation result. The experimental results of nanostructured YBCO filters display lower return losses than the normal YBCO filter prepared from the solid-state thin film. The response of the electrospun filters reflected some of their unique properties of YBCO at the nanoscale, high resistance, large band gap, and low performance. The observed insertion losses could be related to the mismatches and resistance between the contact pads and the electrical contact, which were probably affected by dipping the filter inside the liquid nitrogen [27]. The dimension of the filter is smaller than other previous works reported in open literature [28, 29], and the circuits were fabricated from the conventional YBCO prepared by solid-state and electrospun YBCO. Furthermore, the coupled parallel lines were relatively far apart from each other, and the substrate thickness was very thin, i.e., ~ 0.5 mm.

Table 3 presents the simulated and experimental results for the designed, simulated and measured filters using HTS YBCO thin films deposited by different techniques. The proposed technique and fabricated filters were compared to the ones reported in the open literature [28, 29], which were designed using parallel coupled line and pole. These filters of different substrates, dimensions and YBCO structures (due to various deposition techniques) were simulated with different software [8, 30–32]. Both simulated and measured results in terms of bandwidth, return loss and insertion loss are consistent. The

Table 3. Evaluation summary of the microwave filters designed, simulated and fabricated with different model, Software and synthesize process respectively using superconducting YBCO.

Reference	**Characteristic**				
	Platform for simulation	Filter Design	Substrate	Deposition Process	Dimension (mm^2)
Chung [30]	EM Sonnet	Three parallel coupled H-type	MgO	Pulsed laser deposition	30
Wang et al. [8]	IE3D	Four-pole cross-coupled	$LaAlO_3$	Radio-Frequency Sputtering	225
Shivhare [31]	E6	Four parallel-coupled poles	$LaAlO_3$	Photolithography	254
Zhang et al. [23]	HFSS	Five-parallel pole hairpin	MgO	step-edge junction technology	200
Shang et al. [32]	EM Sonnet	Ten poles	MgO	Photolithography	218
Bai et al. [33]	EM Sonnet	Ten poles	$LaAlO_3$	Photolithography	5898
Bai et al. [9]	EM Sonnet	compact eight-pole	MgO	Photolithography	200
Zhang et al. [28]	EM Sonnet	Parallel-connected network	$LaAlO_3$	magnetron sputtering method	666
Kumar et al. [20]	HFSS	Four parallel-coupled lines	FR4	...	71
Zhang et al. [10]	EM Sonnet	linear phase filter	$LaAlO_3$	Photolithography	425
Liu et al. [34]	EM Sonnet	multi-loop resonators	MgO	...	335
This work	HFSS	Parallel-coupled line	$LaAlO_3$	Electrospinning	100

Reference	**Performance Evolution**							
	Simulation				Experiment			
	Fc (GHz)	BW	RL/dB	IL/dB	Fc/GHz	BW	RL/dB	IL/dB
Chung [30]	16.65	1 GHz	−22	0	16.5	1.35 GHz	−22	−0.5
Wang et al. [8]	2.152	12 MHz	−23.3	0	2.18	9.8 MHz	−5	−1.48
Shivhare [31]	4.035	80 MHz	−20	−0.5	3.7	3.6 GHz	−5.8	−3.5
Zhang et al. [23]	8	2 GHz	−45	−0.5	7.8	2 GHz	−20	−1.2
Shang et al. [32]	10	4 GHz	−20	0	10	2.5 GHz	−14	−0.3
Bai et al. [33]	2.15	0.1 GHz	−20	0	2.15	0.1 GHz	−15	−3
Bai et al. [9]	11	2 GHz	−40	0	11	2 GHz	−40	−0.8
Zhang et al. [28]	2	30 MHz	−25	0	2	30 MHz	−12.5	−0.3
Kumar et al. [20]	2.48	0.6 GHz	−12.5	−2.2	...	...	...	...
Zhang et al. [10]	0.83	10 MHz	−20	0	0.83	10 MHz	−13	−0.3
Liu et al. [34]	1.8	1 GHz	−20	0	1.5	1 GHz	−19	−0.2
This work	10.2	1.5 GHz	−30	0	10.2	1.5 GHz	−15	−1.5

where Fc; Centre of frequency, BW; Bandwidth, RL; Return loss, IL; Insertion loss.

filter developed in the current work has exhibited higher performance (i.e., broad bandwidth, high return loss), although its dimensions are smaller. This result indicates that the filter design is reliable, and it can be adopted in the industry.

5. CONCLUSIONS

In conclusion, an HTS YBCO microwave bandpass filter has been designed and simulated with parallel couple lines model using Ansoft HFSS software. The bandpass filter was fabricated from HTS YBCO thin films prepared by solid state reaction method and electrospinning process. The thin films were deposited double sides on a $LaAlO_3$ substrate ($10 \times 10\,mm^2$). The performance of the HTS YBCO filters was tested using professional network analyzer. The results indicated high-performance device with high return loss $-22\,dB$, broad bandwidth $\sim 1.5\,GHz$, operating frequency of $9.7\,GHz$, which is nearly consistent with the simulation result. The response of the HTS YBCO filter has some insertion loss, which is related to the mismatches of the device with contacts due to dipping in liquid nitrogen. The filter is very small ($100\,mm^2$) with substrate thickness $0.5\,mm$ as compared to other design work. The design and testing of the bandpass filter were compared with other works and showed a high performance and low dimension, attributed to the use of low RF losses HTS YBCO thin films. The filter design and simulation results are reliable, and ensuring transfer the HTS YBCO from lab test to applications.

ACKNOWLEDGMENT

This research is funded by the Ministry of Education Malaysia under the Research Acculturation Collaborative Effort (RACE) grant (Project code: GRS150337).

REFERENCES

1. Nisenoff, M., "Microwave superconductivity Part 1: History, properties and early applications," *2011 IEEE MTT-S International Conference Microwave Symposium Digest (MTT)*, 1–4, 2011.
2. Mansour, R. R., "Microwave superconductivity," *IEEE Transactions on Microwave Theory and Techniques*, Vol. 50, 750–759, 2002.
3. Ribadeneira-Ramírez, J., G. Martínez, D. Gomez-Barquero, and N. Cardona, "Interference analysis between digital terrestrial television (DTT) and 4G LTE mobile networks in the digital dividend bands," *IEEE Transactions on Broadcasting*, Vol. 62, 24–34, 2016.
4. Davidson, D. B., *Computational Electromagnetics for RF and Microwave Engineering*, 23–30, Cambridge University Press, 2010.
5. Newman, N. and W. G. Lyons, "High-temperature superconducting microwave devices: Fundamental issues in materials, physics, and engineering," *Journal of Superconductivity*, Vol. 6, 119–160, 1993.
6. Weigel, R., A. Valenzuela, and P. Russer, "YBCO superconducting microwave components," *Applied Superconductivity*, Vol. 1, 1595–1604, 1993.
7. Van Delft, D., "History and significance of the discovery of superconductivity by Kamerlingh Onnes in 1911," *Physica C: Superconductivity*, Vol. 479, 30–35, 2012.
8. Wang, L., C.-H. Hsieh, and C.-C. Chang, "Cross-coupled narrow-band filter for the frequency range of 2.1 GHz using YBCO resonators with artificial magnetic pinning lattices," *IEEE Transactions on Applied Superconductivity*, Vol. 15, 1040–1043, 2005.
9. Bai, D., J. Du, T. Zhang, and Y. He, "A compact high temperature superconducting bandpass filter for integration with a Josephson mixer," *Journal of Applied Physics*, Vol. 114, 133906, 2013.
10. Zhang, T., K. Yang, H. Zhu, L. Zhou, M. Jiang, and W. Dang, "Miniaturized HTS linear phase filter based on neighboring CQ units sharing resonators," *Superconductor Science and Technology*, Vol. 28, 105012, 2015.

11. Greenberg, Y., Y. Lumelsky, M. Silverstein, and E. Zussman, "YBCO nanofibers synthesized by electrospinning a solution of poly (acrylic acid) and metal nitrates," *Journal of Materials Science*, Vol. 43, 1664–1668, 2008.
12. Shen, Z., Y. Wang, W. Chen, L. Fei, K. Li, and H. L. W. Chan, "Electrospinning preparation and high-temperature superconductivity of $YBa_2Cu_3O_{7-x}$ nanotubes," *Journal of Materials Science*, Vol. 48, 3985–3990, 2013.
13. Duarte, E. A., N. G. Rudawski, P. A. Quintero, M. W. Meisel, and J. C. Nino, "Electrospinning of superconducting YBCO nanowires," *Superconductor Science and Technology*, Vol. 28, 015006, 2014.
14. Cui, X. M., W. S. Lyoo, W. K. Son, D. H. Park, J. H. Choy, and T. S. Lee, "Fabrication of $YBa_2Cu_3O_{7-\delta}$ superconducting nanofibres by electrospinning," *Superconductor Science and Technology*, Vol. 19, 1264, 2006.
15. Uslu, I., M. Kemal Ozturk, M. Levent Aksu, and F. Gokmese, "Fabrication and characterization of boron supported YBCO superconductive nanofibers by electrospinning," *Current Nanoscience*, Vol. 6, 408–412, 2010.
16. Jasim, S. E. and M. A. Jusoh, "Design broad bandwidth microwave bandpass filter of 10 GHz operating frequency using HFSS," *Proceedings of the 119th IIER International Conference*, 31–34, Putrajaya, Malaysia, September 4–5, 2017.
17. Jasim, S. E., M. A. Jusoh, M. Hafiz, and R. Jose, "Fabrication of superconducting YBCO nanoparticles by electrospinning," *Procedia Engineering*, Vol. 148, 243–248, 2016.
18. Chen, J.-X., T. Y. Yum, J.-L. Li, and Q. Xue, "Dual-mode dual-band bandpass filter using stacked-loop structure," *IEEE Microwave and Wireless Components Letters*, Vol. 16, 502–504, 2006.
19. Sun, S. and L. Zhu, "Compact dual-band microstrip bandpass filter without external feeds," *IEEE Microwave and Wireless Components Letters*, Vol. 15, 644–646, 2005.
20. Kumar, M. and S. Kumar, "Designing of half wavelength parallel-edge coupled line bandpass filter using HFSS," *International Journal of Advanced Research in Computer Science and Software Engineering*, Vol. 4, 876–882, 2014.
21. Mohajeri, R., Y. A. Opata, A. C. Wulff, J.-C. Grivel, and M. Fardmanesh, "All metal organic deposited high-Tc superconducting transition edge bolometer on yttria-stabilized zirconia substrate," *Journal of Superconductivity and Novel Magnetism*, Vol. 1, 1–6, 2016.
22. Nur-Akasyah, J., N. Nur-Shamimie, and R. Abd-Shukor, "Effect of CdTe addition on the electrical properties and AC susceptibility of $YBa_2Cu_3O_{7-\delta}$ superconductor," *Journal of Superconductivity and Novel Magnetism*, 1–5, 2017.
23. Zhang, T., J. Du, Y. J. Guo, and X.-W. Sun, "On-chip integration of HTS bandpass and lowpass filters with Josephson mixer," *Electronics Letters*, Vol. 48, 729–731, 2012.
24. Dadras, S. and M. Ghavamipour, "Investigation of the properties of carbon-base nanostructures doped $YBa_2Cu_3O_{7-\delta}$ high temperature superconductor," *Physica B: Condensed Matter*, Vol. 1, 13–17, 2016.
25. Croitoru, M. D., A. A. Shanenko, and F. M. Peeters, "Dependence of superconducting properties on the size and shape of a nanoscale superconductor: From nanowire to film," *Physical Review B*, Vol. 1, 024511, 2007.
26. Lu, X., B. Wei, Z. Xu, B. Cao, X. Guo, and X. Zhang, "Superconducting Ultra-Wideband (UWB) bandpass filter design based on quintuple/quadruple/ triple-mode resonator," *IEEE Transactions on Microwave Theory and Techniques*, Vol. 63, 1281–1293, 2015.
27. Jing, D., K. Shao, C. Cao, L. Zhang, G. Jiao, and Z. Zhang, "10 GHz bandpass YBCO superconducting microstrip filter," *Superconductor Science and Technology*, Vol. 7, 792, 1994.
28. Zhang, T., L. Zhou, K. Yang, C. Luo, M. Jiang, and W. Dang, "The research of parallel-coupled linear-phase superconducting filter," *Physica C: Superconductivity and Its Applications*, Vol. 519, 153–158, 2015.
29. Bhattacharjee, S., D. Poddar, S. Mukherjee, S. Saurabh, and S. Das, "Design of microstrip parallel coupled band pass filter for global positioning system," *Journal of Engineering, Computers &*

Applied Sciences (JEC&AS), Vol. 2, 122–159, 2013.

30. Chung, D.-C., "HTS bandpass filters using parallel coupled microstrip-stepped impedance resonator," *Physica C: Superconductivity*, Vol. 341, 2659–2660, 2000.
31. Shivhare, J., "Design and development of low loss microstrip band pass filters by using YBCO-high temperature superconducting thin film," *Recent Advances in Microwave Theory and Applications, 2008, International Conference MICROWAVE 2008*, 382–383, 2008.
32. Shang, Z., X. Guo, B. Cao, X. Zhang, B. Wei, and Y. Heng, "Design and performance of an HTS wideband microstrip bandpass filter at X-band," *Microwave and Optical Technology Letters*, Vol. 55, 1027–1029, 2013.
33. Bai, D., X. He, X. Zhang, H. Li, Q. Zhang, and C. Li, "Design of an s-band HTS filter with high power capability," *IEEE Transactions on Applied Superconductivity*, Vol. 23, 14–18, 2013.
34. Liu, H., L. Rao, Y. Xu, P. Wen, B. Ren, and X. Guan, "Design of high-temperature superconducting wideband bandpass filter with narrow-band notch resonators for radio telescope application," *IEEE Transactions on Applied Superconductivity*, Vol. 27, 1–4, 2017.